



PERGAMON

Applied Thermal Engineering 19 (1999) 89–115

APPLIED THERMAL
ENGINEERING

Parametric studies on thermally stratified chilled water storage systems

J.E.B. Nelson¹, A.R. Balakrishnan, S. Srinivasa Murthy*

Indian Institute of Technology, Madras - 600 036, India

Received 30 May 1997

Abstract

An analysis of the stratification decay in thermally stratified vertical cylindrical cool storage systems is presented using a one dimensional conjugate heat conduction model. The degree of thermal stratification depends upon the length to diameter ratio, wall thickness to length ratio, the thermo-physical properties of the material of the storage tank, the type and thickness of the insulation and the design of the admission system for both cold and warm water. A parametric study of the stratified chilled water storage tanks in charging, discharging and stagnation modes of operation is made. The thermoclines degrade due to the heat transfer from the ambient, thermal diffusion in the storage tank, axial wall conduction and mixing due to admission of the fluid in the storage tank during charging and discharging. The degree of thermal stratification in storage tanks is expressed in terms of either heat capacity (thermal capacitance ratio) or modified Biot Number. A mixing parameter accounts for the effect of mixing on thermal stratification in both charge and discharge cycles. © 1998 Elsevier Science Ltd. All rights reserved.

Keywords: Thermal stratifications; Mixing parameter; Chilled water; Axial conduction

Nomenclature

A	Cross sectional area of the storage tank, m ²
A_s	Surface area of the storage tank, m ²
A_r	Aspect ratio (L/D)
$a_{1,2}$	Constants

* Author to whom correspondence should be addressed.

¹ Present address: Dept. of Mechanical Engg., Regional Engg. College, Warangal - 506 004, India.

Bi	Biot number
Bi_m	Modified Biot number
c	Specific heat, $\text{kJ kg}^{-1} \text{K}^{-1}$
$C_{1..8}$	Heat capacity of storage fluid, kJ K^{-1}
D	Diameter of the storage tank, m
F	Dimensionless initial temperature, $F(X) = \{T - T_\infty\} / \{T_{in} - T_\infty\}$
h	Heat transfer coefficient, $\text{W m}^{-2} \text{K}^{-1}$
k	Thermal conductivity, $\text{W m}^{-1} \text{K}^{-1}$
L	Length of the storage tank, m
Nu	Nusselt number, (hL/k_f)
P	Perimeter of the tank, m
Pe	Peclet number, (vL/α_f)
q	Length to diameter ratio of the storage tank, (L/δ)
r	Specific heat capacity ratio of fluid and tank material, $\rho_f C_f / \rho_w C_w$
S	Heat loss coefficient inside the tank, $S_{i(o)} = 4 Nu_{i(o)} A_r$
s	Thermal conductivity ratio, k_f/k_w
T	Temperature of water, $^\circ\text{C}$
T_w	Temperature of wall, $^\circ\text{C}$
V	Volume of the storage tank, m^3
v	Average bulk velocity, m s^{-1} ($m/A\rho_f$)
X	Dimensionless axial coordinate, x/L
x	Axial co-ordinate, m
$Z_{1..8}$	Mixing parameters at extreme nodes (top and bottom)
Z_{int}	Mixing parameters at the inner nodes

Greek letters

α	Thermal diffusivity, $\text{m}^2 \text{s}^{-1}$
θ	Non-dimensional temperature, $\theta = \{T - T_\infty\} / \{T_{in} - T_\infty\}$
ρ	Density, kg m^{-3}
δ	wall thickness of the storage tank, m
ε	Heat capacity ratio of the stored fluid and storage tank

Subscripts

b	bottom
i	inside, in
o	outside
t	top
w	wall
∞	Ambient

1. Introduction

Comfort cooling contributes to a major portion of the summer electricity demand. Unlike other uses of electricity, cooling goes through a peak demand for only a few months in a year. The storage of cooling effect is an option to shift the electrical demand in commercial buildings in which significant cooling loads occur during electric utility peak periods. The storage systems also enable the users to reduce their electric demand charges where differential tariff

rates prevail. The integration of a thermal storage into the existing cooling system allows it to meet the requirements of expanded cooling capacities. In addition to the above, the use of a thermal storage increases the overall efficiency of the chilled water plant.

Since there is a mismatch between the times of production and the usage of chilled water, the thermal energy storage system should be designed to have minimum loss or degradation of stored energy when the storage tank is left idle. Further, a chilled water storage is based on maintaining a thermal separation between cool charged water and warm return water. There are various methods of separating the warm and cold water in the same tank. Thermally stratified storage systems take the advantage of temperature dependence of water density to store both warm and cold water in a single tank. A large temperature gradient exists in the interface separating the warm and cold water. This small thickness of interfacial zone is called a thermocline. In a well designed stratified storage system the thickness of this thermocline zone should be very small. The erosion in the thermocline results in the loss of available cooling energy.

The performance of the stratified storage is influenced by several factors such as the operating temperature range, thermo-physical properties of the storage fluid and storage tank material, geometry of the storage tank, methods of admission and withdrawal of stored fluid and heat transfer between the storage tank and outside environment.

There have been several studies in the literature to analyze thermal stratification in a hot water storage. However thermally stratified cool storages have not been widely studied.

Fiorino [1, 2] has made a case study of a large naturally stratified chilled water storage system. Their study has proved that thermal energy storage is a reliable cost-effective means of conserving energy and reducing facility's annual energy costs.

Gretarson *et al.* [3] have developed a time step model to study the performance of cool storages. Their numerical model solves the one dimensional transient heat transfer equation using Runge–Kutta method for obtaining time dependent tank water temperatures. They introduced a discrete time step concept to account for the convective flow through the tank. Their model needs an appropriate time scaling to achieve stability in computation. They have performed a parametric study to investigate the overall effects of neglecting the thermal mass of the tank walls, in a storage tank of aspect ratio of unity. They have observed that in tanks whose wall thermal capacitance to water thermal capacitance ratio is less than 0.2 the discrepancy in the values of internal energy between calculated and experimental results is less than 3%.

Truman and Wildin [4] have used an explicit finite difference numerical model to analyze the performance of the stratified storage systems. Their model solves a two dimensional transient heat conduction equation in the wall and one dimensional heat conduction in the tank fluid to predict the temporal and spatial variations in the tank fluid. Their experimental temperature profiles are made to agree with their numerical results by using outer wall resistances which are half of the actual wall resistances.

Yoo and Pak [5] have developed a theoretical model of the charging process for stratified thermal storage tanks used in solar applications. They have obtained a closed form solution for the transient temperature distribution of the stored fluid in the tank, using Laplace Transform technique. Their model has been validated with a simple alternative model, which is heat conduction between two semi-infinite regions in contact with an interface moving at constant

velocity. They characterized only one parameter Peclet Number in controlling the thermal stratification and discussed its effect on the temperature profiles. The storage efficiency is expressed by a simple correlation. The limitation of their model is that it can be used only for studying the performance of the hot water storage tanks during charging process.

Al-Nimr [6] has developed a mathematical model for the conjugate behaviour of a hot water storage tank having finite wall thickness. He has obtained a closed form analytical solution for the temperature field within the tank using Laplace transform technique. The solution takes into account the axial conduction within the fluid and tank wall and the heat capacity of the storage tank wall. He has observed the thermal stratification to decrease with finite wall thickness, and this effect to become less apparent at high Peclet Numbers. This model also deals with only the charging process.

Many of the one dimensional models, though they are simple, involve using several empirical constants to account for mixing, axial wall conduction etc. in the evaluation of the performance of the storage systems. Two and three dimensional models are complex, difficult to solve and are unsuitable for use in large energy system simulation programs.

In this paper, a one dimensional transient heat transfer model which takes into account the effects of axial conduction, the physical properties of the storage tank wall, fluid, dimensions of the storage tank and the mixing effects due to in-flow and out-flow of the stored fluid in the tank is developed. This model is used for predicting the temperature profiles in the fluid and tank wall under both static and dynamic mode of operation. The four heat transfer mechanisms which control the thermocline degradation in the storage systems, i.e. heat leaks from the ambient, conduction through thermocline, conduction from warm fluid layers to cold fluid layers through the conducting wall and thermal mixing at inlet and outlet, are taken into account.

2. Analysis

The physical system considered in this analysis is shown schematically in Figs. 1 and 2. The cylindrical tank is divided into N equal elements in the longitudinal direction. The initial temperature profile in the tank is known. An energy balance on an elemental volume gives the governing differential equation for this one-dimensional transient conduction problem. The energy balance in the fluid and wall at a distance x from the top of the tank (Fig. 1) are given by:

$$\frac{\partial T}{\partial t} = \frac{k_f}{\rho_f c_f} \frac{\partial^2 T}{\partial x^2} - \frac{\dot{m}}{\rho_f c_f} \frac{\partial T}{\partial x} + \frac{h_i P}{A_f \rho_f} (T_w - T), \quad (1)$$

where \dot{m} is the charge or discharge rate:

$$\frac{\partial T_w}{\partial t} = \alpha_w \frac{\partial^2 T_w}{\partial x^2} + \frac{h_o P}{A_w \rho_w c_w} (T_\infty - T_w) - \frac{h_i P}{A_w \rho_w c_w} (T_w - T). \quad (2)$$

The initial conditions in the fluid and wall are:

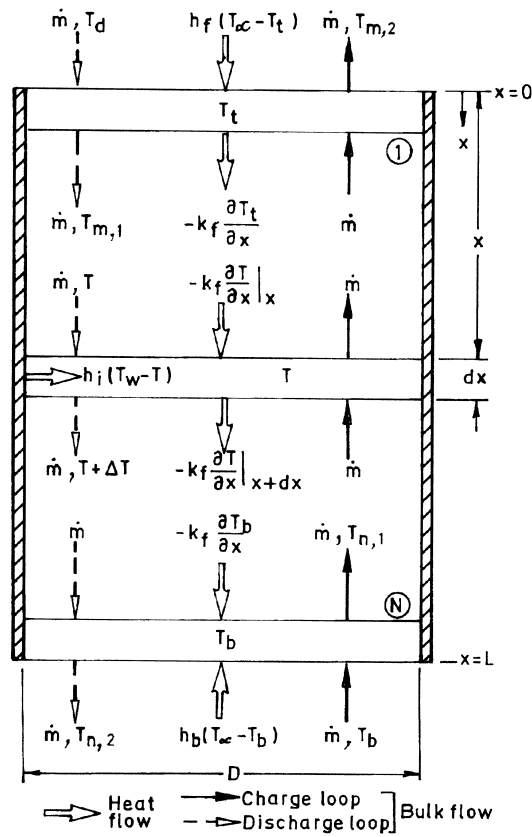


Fig. 1. Schematic diagram of stratified storage tank.

$$\theta(x, 0) = F(x), \tag{3}$$

$$\theta_w(x, 0) = F_w(x). \tag{4}$$

The boundary condition at $x = 0$ in the charge cycle is:

$$\frac{\partial T_t}{\partial x} + \frac{h_t}{k_f} (T_\infty - T_t) + \frac{\dot{m} c_f}{K_f A} (T_d - T_{m,1}) = 0. \tag{5}$$

The boundary condition in the discharge cycle at $x = 0$ is:

$$\frac{\partial T_t}{\partial x} + \frac{h_t}{k_f} (T_\infty - T_t) + \frac{\dot{m} c_f}{K_f A} (T_t - T_{m,2}) = 0. \tag{6}$$

In the static mode the second and third terms in Eqs. (5) and (6) are zero for insulated boundary condition and for convective boundary condition the third term alone is zero.

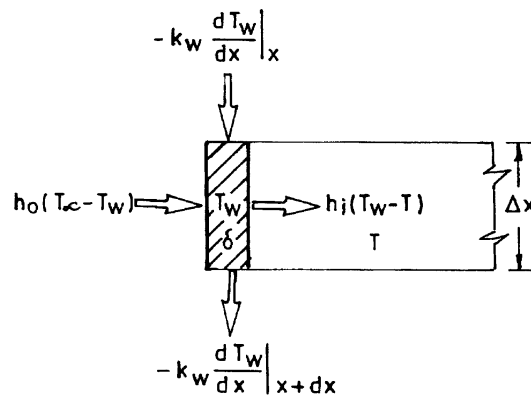


Fig. 2. Energy flow diagram in stratified storage tank.

The boundary condition in the discharge cycle at $x = L$ is:

$$\frac{\partial T_b}{\partial x} - \frac{h_b}{k_f} (T_\infty - T_b) - \frac{\dot{m} c_f}{K_f A} (T_N - T_{n,2}) = 0. \quad (7)$$

The boundary condition at $x = L$ in the charge cycle is:

$$\frac{\partial T_b}{\partial x} - \frac{h_b}{k_f} (T_\infty - T_b) - \frac{\dot{m} c_f}{K_f A} (T_u - T_{n,1}) = 0. \quad (8)$$

The second and third terms in Eqs. (7) and (8) are zero for insulated boundary condition and for convective boundary condition the third term alone is zero.

The boundary conditions in the wall are:

$$\frac{\partial T_w}{\partial x} = 0 \quad \text{at } x = 0 \quad \text{and } x = L. \quad (9)$$

3. Method of solution

The governing Eqs. (1) and (2) which are linear partial differential equations are nondimensionalized. (The nondimensionalized form of the equations are shown in the Appendix).

The convection term in the nondimensionalized form of Eq. (1) (equation (A.19)) is converted into finite difference equation using Upwind difference scheme and the diffusion terms in nondimensionalized form of Eqs. (1) and (2) (equation (A.19) and (A.20)) are converted using Central difference scheme. The numerical diffusion due to convective term is thus taken care of using the Upwind difference scheme. The converted finite difference equations are simultaneously solved, using Crank-Nicolson Implicit Finite Difference scheme, subject to initial and boundary conditions as shown in equations from (3) to (9). (Nondimensionalized equation (A.21) to (A.27) for various modes of operation. For stability

the time step must be smaller than $(\Delta x^2/2 \alpha_f)$. The error in time step is of the order (Δt) and space step is of the order of (Δx^2) . A time step of 0.01 s is taken here to satisfy the stability condition of the numerical scheme.

The inputs to the program include operating conditions (initial temperature difference and flow rate), thermophysical properties (for water and tank material) and dimension (length, diameters, wall thickness).

A mixing coefficient takes into account the effects of mixing during both charging and discharging cycles. A correlation developed based on extensive experiments by the authors [7] is used as follows.

$$Z = 1.688 \times 10^4 \left(\frac{Re}{Ri} \right)^{0.67} . \quad (10)$$

4. Results and discussion

A parametric study of the stratified chilled water storage system enables one to identify the factors responsible for the degradation of available cooling capacity of a stratified cool storage. The operational and system parameters affecting the thermal stratification are expressed as dimensionless numbers.

In this study the following values and ranges of parameters are considered.

Warm water temperature	15°C
Chilled water temperature	5°C
Aspect ratio (A_r)	2 to 3.5 in steps of 0.5
Length to wall thickness ratio (L/δ)	50 to 300
Flow rates	45 to 1440 l/h
Initial temperature difference	5 to 10°C

The above parameters are selected based on the practices followed in comfort air conditioning of buildings, using chilled water systems.

4.1. Static mode

In this mode of operation the storage tank which is initially at uniform temperature of 15°C is assumed to have been stratified with chilled water at 5°C to half the height. The storage system is allowed to settle down. The temporal and spatial temperature profiles of the fluid and wall are predicted using the numerical model. The parameters affecting the thermal stratification in this mode of operation are: aspect ratio of the storage tank, length to wall thickness ratio of the storage tank, tank wall material and external heat transfer resistance of the tank.

The effect of aspect ratio on thermal stratification in storage tanks under static stratified mode is considered here under three different cases. The storage tanks are assumed to be made

of the same material, and provided with the same insulation thickness in all the three cases under study.

4.2. Case 1. Tanks of the same diameter and wall thickness but of different lengths

Figure 3 shows the temperature profiles for a time interval of 6 h in four storage systems of the same diameter, wall thickness, surface area to volume ratio, heat capacity ratio, external insulation resistance and wall material, but of different lengths giving aspect ratios of 2, 2.5, 3 and 3.5. The initial temperature distribution is the same in all cases. The length to wall thickness ratio, and the volume of the above storage tanks also vary in the ratio of 2.0, 2.5, 3.0 and 3.5. The rate of warming up of the stored fluid due to energy transfer from the ambient is the same in all the tanks. Thermal diffusion within the fluid depends on the temperature difference between warm and cold layers of water. The thermal diffusion decreases with the increase in the length of the tank. The thermal inertia of the wall is the same in all four storage tanks. Obviously the axial wall conduction decreases with the increase in the length of the storage tank.

A dimensionless parameter, called modified Biot number (Bi_m) is defined to account for the axial conduction effect in expressing the degree of thermal stratification. This parameter compares the heat convected through the walls to the heat conducted longitudinally (axial conduction) and is given as:

$$Bi_m = \frac{h_o L^2}{k_w \delta} = \frac{h_o \pi D L \Delta T_f}{k_w \pi D \frac{\delta}{L} \Delta T_w} \quad (11)$$

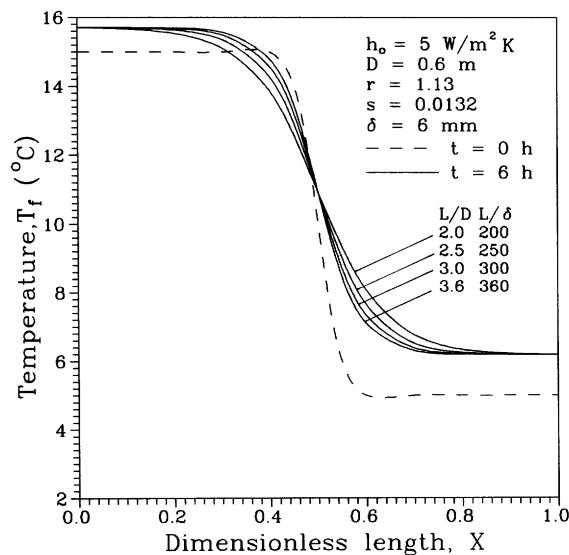


Fig. 3. Effect of aspect ratio on thermal stratification in static mode in storage tanks of the same diameter and different lengths.

When the modified Biot Number is small, the energy conducted through the wall is more than the energy converted out through the walls. Hence, the temperature of the storage tank walls will be higher than the fluid temperature in the coldest part of the storage tank. This result in the warming up of the cold water layers at the bottom. The energy conducted through the wall decreases with increase in the length of the tank (L) or decrease in the value of wall thickness (δ). Hence the axial wall conduction decreases with the increase in the value of Bi_m . The modified Biot number of the storage tanks in this case increases with the increase in the aspect ratio. So the degree of thermal stratification increases with increase in the aspect ratio in storage tanks having the same diameter and wall thickness. Thus, the higher the modified Biot number the better will be the thermal stratification in storage tanks of the same heat capacity, surface area to volume ratio and external insulation resistance.

4.3. Case 2. Tanks of the same length, wall thickness but different diameters

In this case four storage systems of the same length, wall thickness, external insulation resistance and wall material are considered. The diameters of these tanks are so chosen as to give aspect ratios of 2, 2.5, 3 and 3.5. Results for these tanks are shown in Fig. 4. The surface area to volume ratios (A_s/V) of the above storage tanks increase with increase in the aspect ratio. The rate of warming up of the stored fluid is proportional to surface area to volume ratio of the storage tank. Another parameter which controls the degradation of thermoclines is the heat capacity ratio. When the heat capacity of the storage tank is much smaller than the heat capacity of the fluid in the tank, wall effect on thermocline degradation is negligible. The increase in the surface area to volume ratio and the decrease in the heat capacity ratio with increase in aspect ratio, both contribute to increase in thermal degradation. The modified Biot

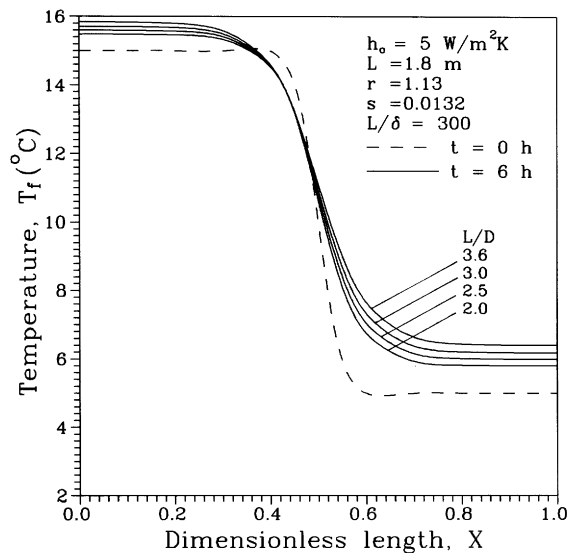


Fig. 4. Effect of aspect ratio on thermal stratification in static mode in storage tanks of the same length but different diameters.

Numbers of these tanks are the same since L and δ are constant and D alone varies with the aspect ratio. The initial temperature distribution in the fluid and wall is assumed to be the same in all the storage tanks. The temperatures of the bottom layers of chilled water and the upper layers of warm water increase as time elapses. This effect is observed to increase with increase in the aspect ratio of the storage tank. The trend in the above figure are the opposite to those in Fig. 3. The bottom layers of chilled water heat up more showing increased thermal degradation at any aspect ratio. In the case of storage tanks of large storage volumes and when there is a restriction on the maximum length of the storage tank, it is possible to produce thermal stratification even at low aspect ratios by maximising the heat capacity ratio and minimising the surface to volume ratio.

4.4. Case 3. Tanks of the same diameter, but different lengths and wall thicknesses

Figure 5 shows the temperature profiles in storage systems made of the same wall material and of same diameter. The length and the wall thickness of the storage tanks are so chosen to give different aspect ratios of 2, 2.5, 3.0 and 3.5. In Case 1 the wall thickness of all the storage tanks were maintained constant. The wall thicknesses are so chosen as to give the same L/δ ratio for all the storage systems. The initial temperature distribution and the surface area to volume ratio are the same in all the four storage systems. The rate of warming up is the same in all the storage tanks. The modified Biot numbers of these storage systems increase with increase in the aspect ratio of the storage tank (see Eq. (11)). Hence the thermal stratification increases with modified Biot Number. The degree of thermal stratification does not improve appreciably beyond an aspect ratio of 3.0, as seen from the temperature profiles. Figs. 5 and 3 refer to the thermoclines in storage tanks of the same geometrical and operating conditions

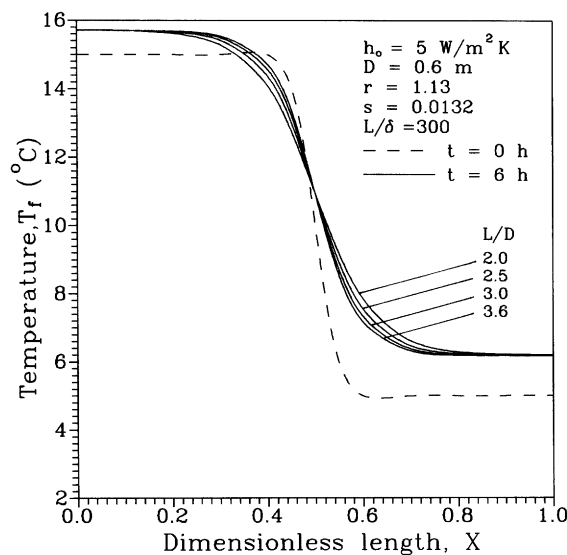


Fig. 5. Effect of aspect ratio on thermal stratification in static mode in storage tanks of same diameter, same L/δ and different lengths.

except that in the former L/δ is constant and in the later it varies due to change in δ only. A close observation of the above figures shows that thermal stratification is better in the former at any aspect ratio.

The effect of L/δ on stratification is studied in four different storage tanks having the same diameter, length, external insulation resistance and wall material, but different wall thicknesses. The effect of L/δ on thermal stratification is studied in storage tanks having the same diameter, length, external resistance and wall material, but different wall thicknesses. The heat capacity ratio and modified Biot number increases with L/δ . Both of these have the effect in lowering the thermal degradation due to axial wall conduction. Hence thermal stratification increases with L/δ as seen in Fig. 6. No significant thermal stratification is observed at L/δ greater than 200.

The effect of the wall material on thermal stratification is studied in four geometrically similar storage tanks, made of different materials. The temperature profiles of the stored fluid in these tanks are plotted in Fig. 7. It is observed that the thermal stratification improves with the increase in the modified Biot Number. The value of the modified number decreases with increasing thermal conductivity. Hence, thermal stratification improves for aluminum, mild steel, stainless and fibre glass tanks in that order.

A large external conductance (Nu_o) results in increased heat flux transmitted from the ambient leading to faster degradation of thermoclines. Figure 8 represents the temperature profiles computed for two geometrically similar mild steel tanks of different external insulation resistances.

Figure 9 represents temperature profiles at two time intervals for two initial temperature differences in the tank. The increase in initial temperature difference helps in producing stable thermoclines during their formation due to increased density difference. However this has the

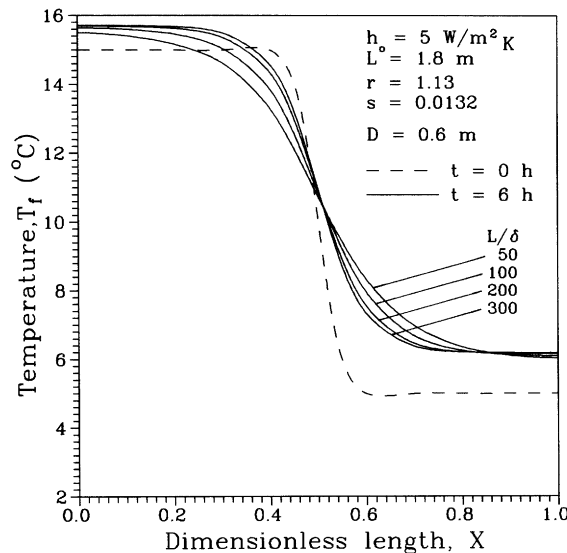


Fig. 6. Effect of L/δ on thermal stratification in static mode.

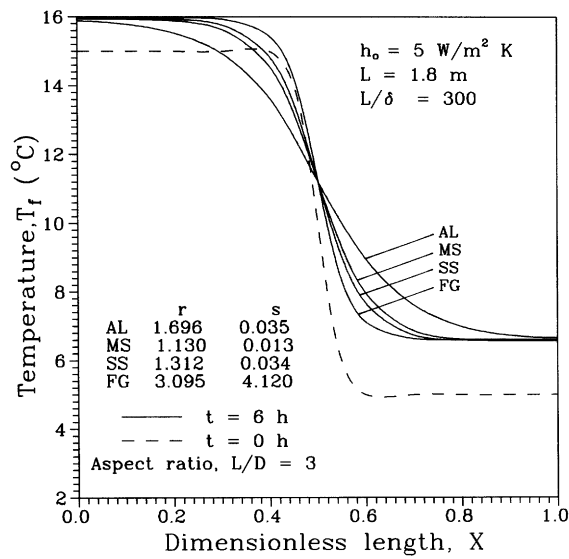


Fig. 7. Effect of tank wall material on thermal stratification in static mode.

adverse effect of increasing the rate of thermal degradation due to axial wall conduction and thermal diffusion. It is noticed that thermocline formation will be easy at an initial temperature difference of 15°C in the temperature ranges applicable in chilled water systems used for comfort cooling.

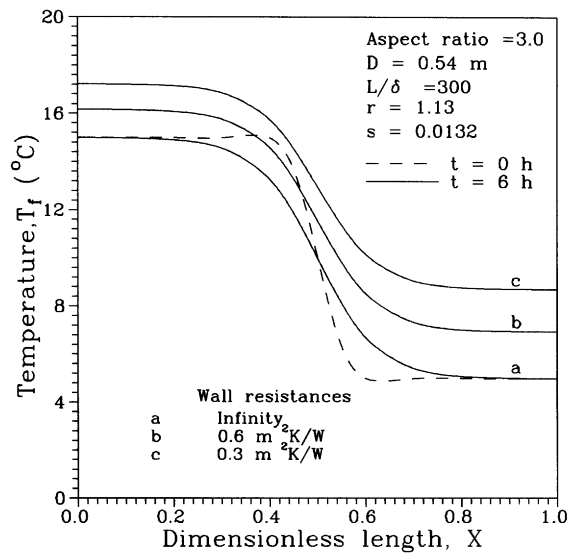


Fig. 8. Effect of wall conductance on thermal stratification in static mode.

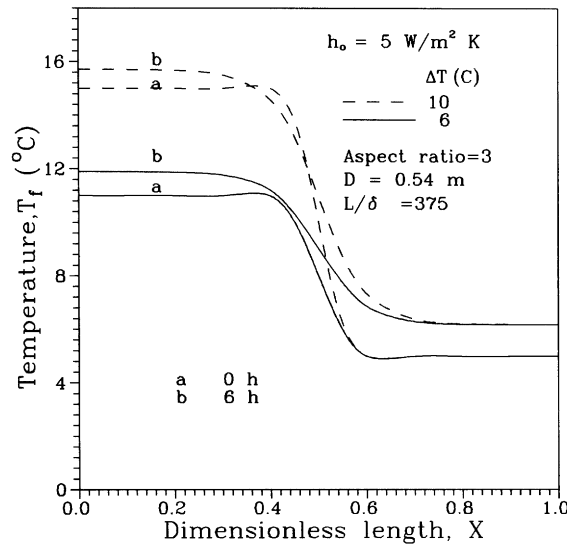


Fig. 9. Effect of initial temperature difference on thermal stratification in static mode.

4.5. Dynamic mode

In the dynamic mode the stratified cool storage system is analyzed for its performance both in charge and discharge cycle operations.

4.5.1. Charge cycle

The charge cycle is simulated by assuming the storage system to be initially at a uniform temperature, the chilled water is admitted through the diffuser at the bottom of the tank at the same rate as the warm water is withdrawn through the top of the tank. The diffuser helps in admitting the water with minimum flow disturbance and thus reduces the tendency of blending of warm and chilled water in the storage tank.

The effect of flow rate on stratification is shown by drawing the transient temperature profiles for the same amount of water charged into the tank. The degree of thermal stratification is expressed in terms of the dimensionless parameter, Peclet Number, which represents the ratio of the energy added to the tank by the fluid flowing through it to the rate of heat conduction through the thermocline. The time required for completely charging the tank is called the turn-over time. The turn-over time decreases with increase in the flow rate (Peclet Number). Figure 10 shows the temperature profiles at various time intervals during the charging process. The thermocline forms initially when chilled water enters the tank. The thermocline thickness increases as the charging is continued. This is mainly due to the heat conduction across the thermocline, axial wall conduction and mixing at the inlet port.

Figure 11 shows the temperature profiles for four different flow rates at $Pe \cdot Fo = 0.5$. The product of Peclet number and Fourier number denotes the ratio of the volume of water charged or discharged in a given time to the total volume of the storage tank. This also

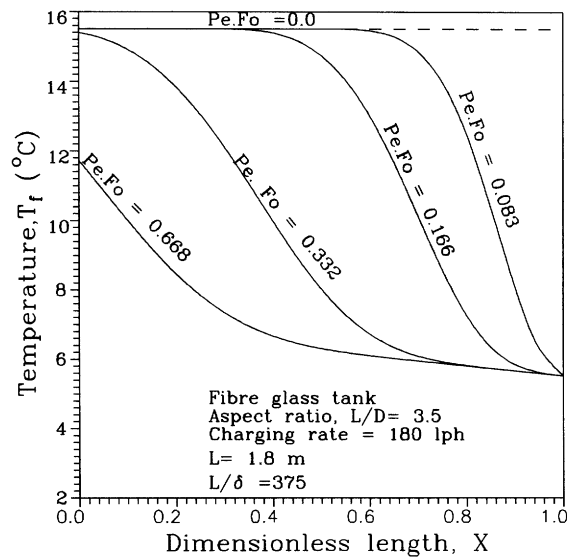


Fig. 10. Transient temperature profiles during the charge cycle.

represents the fraction of the turn-over time to a different scale. The results reveal that the thermocline degradation is more pronounced at low flow rates. Thermal diffusion, axial wall conduction and heat exchange with the ambient are rate processes. The energy degradation due to these is directly proportional to the charging time. Hence the degradation of energy due to heat conduction across the thermocline and along the storage tank (axial wall conduction) increases with the increase in charging time, i.e. at low flow rates. Stratification improves with

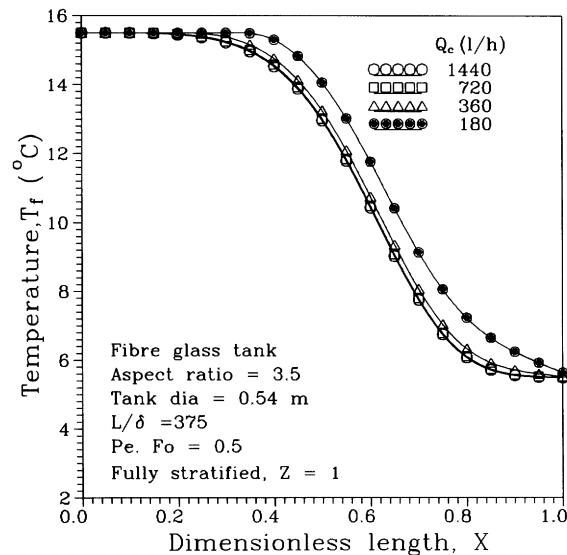


Fig. 11. Effect of flow rate on thermoclines during charge cycle.

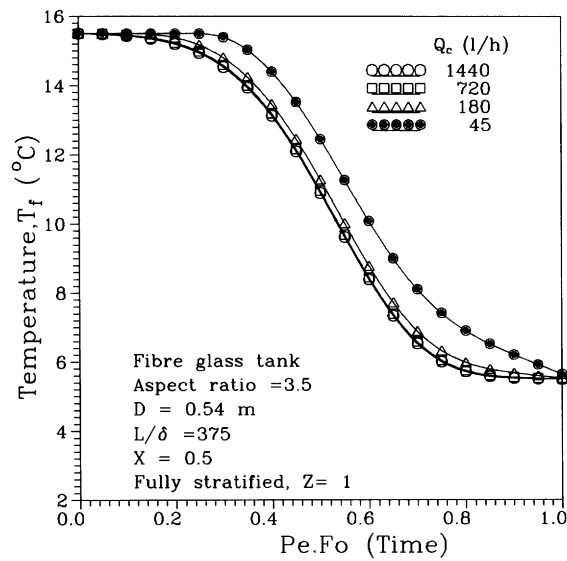


Fig. 12. Effect of flow rate on thermocline at $X = 0.5$ during charge cycle, without mixing.

increasing flow rate up to a certain value and there after remains constant. Figures 12 and 13 represent the effect of Peclet number on temperature variation with time at $X = 0.5$. The thermocline degradation increases with decrease in the Peclet number due to the same reasons as explained above. Figure 14 represents the thermoclines in three geometrically similar storage tanks made of different materials and insulated with the same type and thickness of insulation. It is observed that the tank wall material does not have much influence in the thermocline

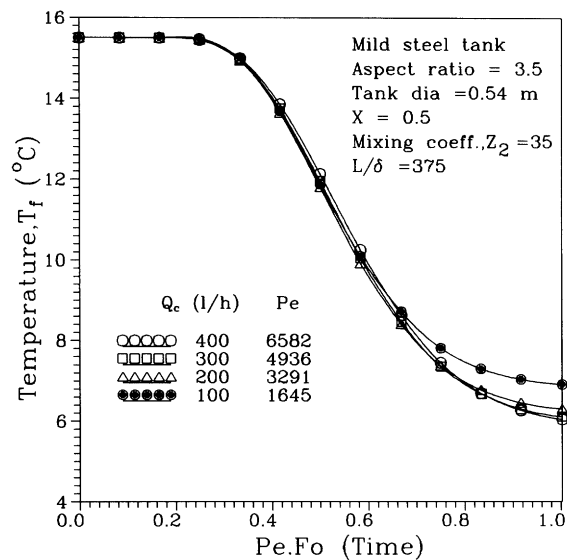


Fig. 13. Effect of flow rate on thermocline at $X = 0.5$ during charge cycle, with mixing.

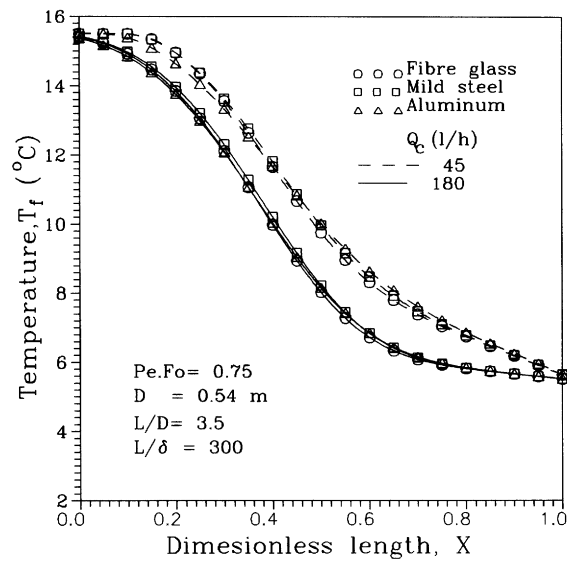


Fig. 14. Effect of wall material on thermal stratification during charge cycle.

formation and degradation. For the large L/δ ratio of 300 considered in the above cases, which denotes a relatively thin wall, there is very little difference in the axial conduction between the various storage systems.

Figures 15 and 16 show the effect of aspect ratio on the thermal stratification during charging. The effect of aspect ratio is studied in two different cases:

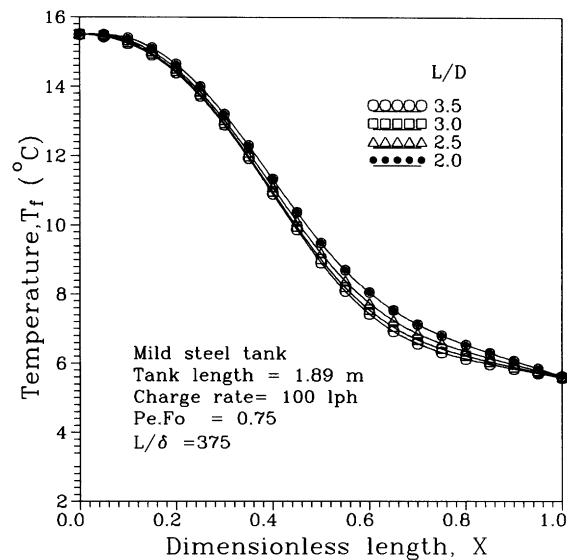


Fig. 15. Effect of aspect ratio on thermoclines during charge cycle in storage tanks of different diameters.

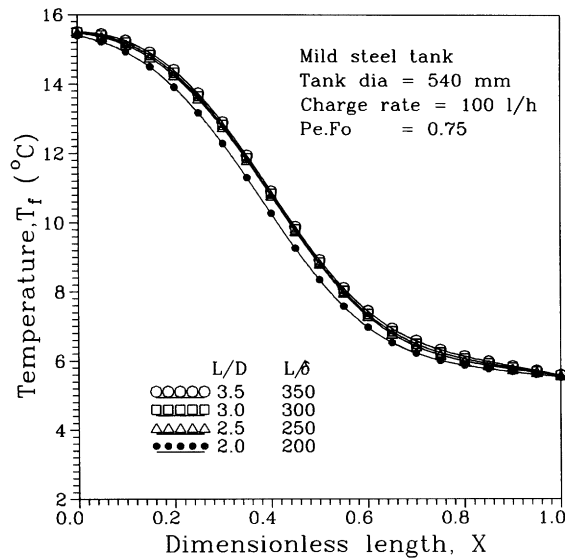


Fig. 16. Effect of aspect ratio on thermoclines during charge cycle in storage tanks of different lengths.

4.5.2. Case i. Tanks of the same length, wall thickness but different diameters

In this case four storage tanks of equal lengths but different aspect ratios are studied. The charging time increases with the decrease in the aspect ratio of the tank. The surface area to volume ratio decreases with the decrease in the aspect ratio. The axial conduction effect is the same in all the storage tanks. The increase in charging time increases the energy degradation due to thermal diffusion and axial conduction. The rate of warming up due to energy transfer from the ambient decreases with the decrease in the aspect ratio. The loss in available cooling due to thermal diffusion and axial wall conduction increases with the increase in the charging time in tanks of low aspect ratio. But this increase in the loss of available cooling is larger than the reduction in the loss of available cooling due to reduction in the surface area to volume ratio of the storage tanks with low aspect ratio. Hence the thermal stratification increases with decrease in the aspect ratio of the tank as shown in Figure 15.

4.5.3. Case ii. Tanks of same diameter but different lengths

In this case the surface area to volume ratio in all these tanks is the same. Hence the rate of degradation of thermoclines due to energy transfer from the ambient is the same in all the storage tanks. The axial wall conduction decreases with the increase in the aspect ratio. The net loss in available cooling due to thermal diffusion, axial wall conduction, heat transfer from the ambient increases with the charging time, which decreases with the aspect ratio. Hence the thermal stratification decreases with increase in the aspect ratio of the storage tank. However, for the parameter values considered, this variation is not significant as seen in Figure 16.

Fig. 17 represents the thermoclines in two geometrically similar stratified storage tanks charged at the same flow rate, but with different initial temperature differences of 10°C and 5°C. The thermocline degradation increases with the increase in the initial temperature difference. Even though large initial temperature difference helps in producing stable

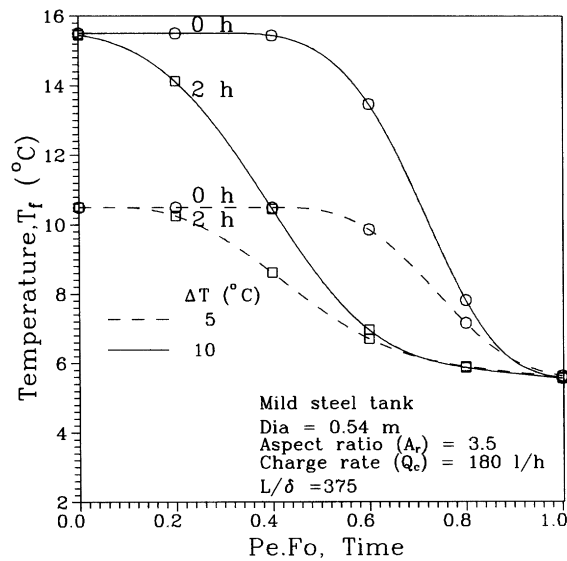


Fig. 17. Effect on initial temperature difference of thermal stratification during charge cycle.

thermoclines, due to increased density difference, the rate of degradation of thermoclines, is found to increase with initial temperature difference due to increased energy transfer across the thermocline and along the tank wall.

4.5.4. Discharge cycle

A chilled water storage is normally charged at the coldest possible temperature above 4°C. Water is at its maximum density at 4°C and water introduced into a stratified tank below this temperature floats upward causing unwanted mixing. The maximum storage capacity is obtained when the storage is charged at 4°C. The water should be sent to the tank at a constant temperature to avoid short-term density differences that cause buoyancy currents at the diffuser. Stored water increases in its temperature slightly due to conduction heat gains and unavoidable mixing. The discharge temperature gradually rise through the discharge period, increasing more rapidly at the end of the discharge period. The temperature rise during the discharge depends on the quality of stratification within the storage tank. This in turn depends on the diffuser design, heat transfer within the tank and through the tank walls.

In the discharge cycle the tank is initially assumed to be full with chilled water, is discharged through the bottom at the same rate as the return warm water from load is charged through the diffuser at the top of the tank. The transient temperature distribution in the fluid during the discharge cycle is shown in Fig. 18. The thermocline forms at the top of the storage tank as soon as the warm water enters the tank from the load through the diffuser at the top of the tank. The thermocline thickness increases with time. Figure 19 shows the time-wise variation of temperature at various axial locations in a discharge cycle. $X = 1.0$ refers to the bottom of the storage tank. The temperature of this layer slowly increases with the turn-over time ($Pe \cdot Fo$) as seen from Fig. 19. The discharge temperature slowly increases with time. This increase in discharge temperature results in the loss of available cooling.

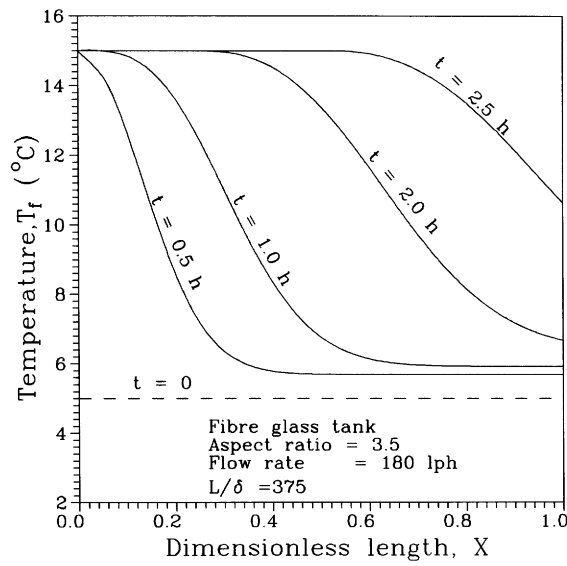


Fig. 18. Transient temperature profiles during discharge cycle.

Figure 20 shows the axial variation in temperature of the stored fluid for four different Peclet Numbers (flow rates). The time taken to discharge the given volume of water decreases with increase in the flow rate of water. The bottom layers of chilled water warm up due to conduction across the thermoclines and axial wall conduction. The time for discharging the tank increases with the decrease in the flow rate of water. This results in increased energy transfer between the warm and chilled water due to conduction across the thermoclines and

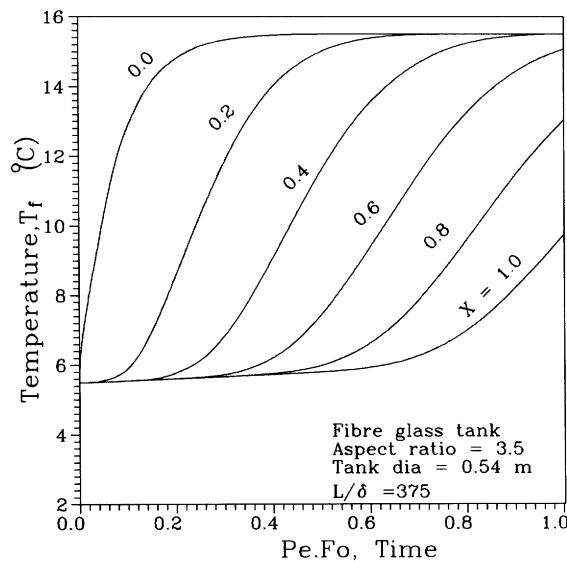


Fig. 19. Temperature profiles at various axial locations.

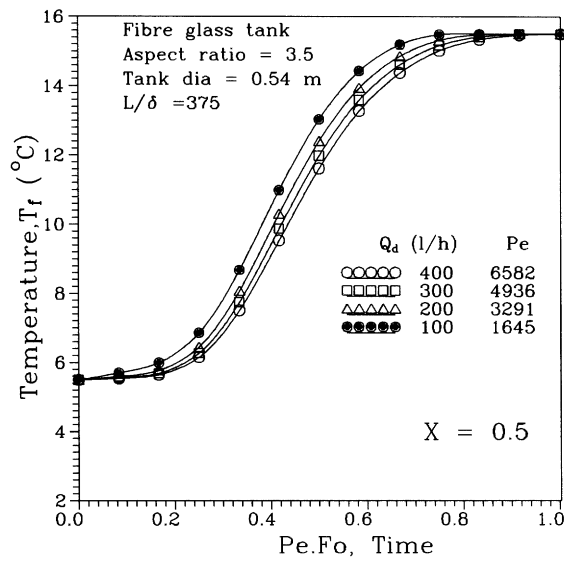


Fig. 20. Effect of flow rate on temperature profiles at $X = 0.5$ during discharge cycle.

along the tank wall. The thermocline degradation is more at low flow rates due to increase in the discharging time.

Figure 21 shows the temperature profiles in three geometrically similar storage tanks made of glass fibre, mild steel and aluminum. All three storage tanks are insulated with the same insulation material and to the same extent. The discharge rate is the same in all three cases. The thermal degradation in these tanks due to thermal diffusion, heat gain from ambient and

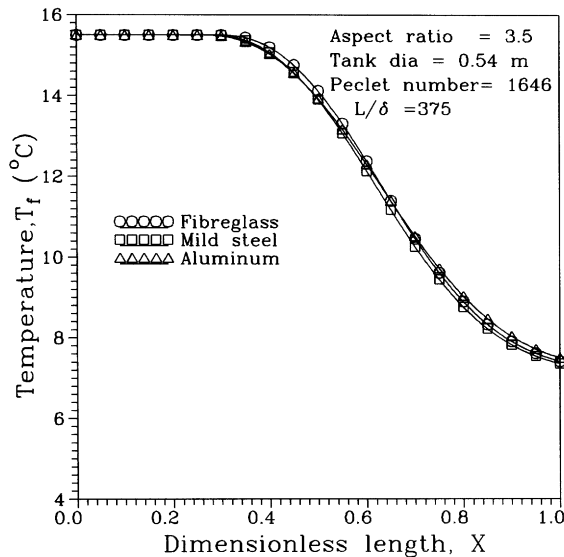


Fig. 21. Effect of wall material on thermal stratification during discharge cycle.

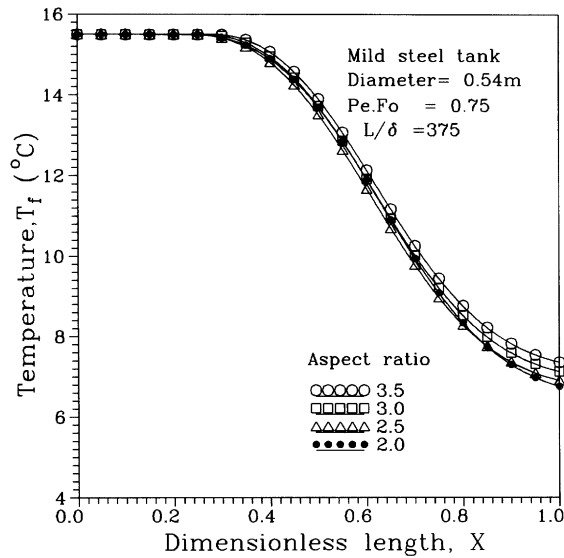


Fig. 22. Effect of aspect ratio on thermal stratification during discharge cycle in storage tanks of different diameters.

mixing are the same. The degradation due to axial wall conduction depends on the thermal conductivity of tank wall material and L/δ ratio. A large L/δ ratio used shows that the variation in the axial conduction in these tanks is small. Hence the temperature profiles show that the tank wall material has very little influence on the thermocline formation and maintenance during discharging.

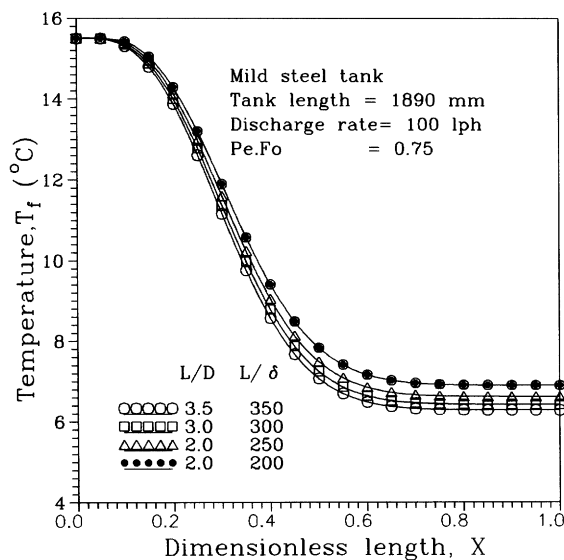


Fig. 23. Effect of aspect ratio on thermal stratification during discharge cycle in storage tanks of different lengths.

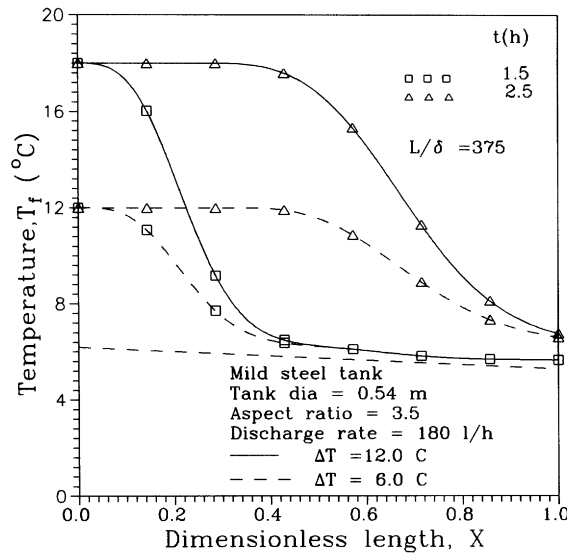


Fig. 24. Effect of initial temperature difference on thermal stratification during discharge cycle.

Figure 22 represents the thermoclines in storage tanks of the same diameter but different lengths to give different aspect ratios. The axial wall conduction increases with the decrease in the aspect ratios of the tank. The discharging time increases with the increase in the aspect ratio. The loss in available cooling increases with the increase in discharging time as the energy transfers are all rate processes. The temperature profiles drawn in the above figure show that thermocline degradation is more in tanks of large aspect ratios due to increase in discharge time for the same volume of water discharged from the tank. The discharge temperatures of the water (temperature of the water at $X = 1$) is low in tanks of low aspect ratio. However, for the parameter values considered, this variation is not significant as seen in Fig. 22.

Figure 23 represents the thermoclines in tanks of different aspect ratios, having the same length. The surface area to volume ratio decreases with decrease in the aspect ratio of the storage tank. The axial wall conduction increases with the decrease in the length of the storage tank. The discharging time increases with the decrease in the aspect ratio of the storage tank. The increase in the loss in available cooling capacity due to increase in axial wall conduction dominates the reduction in the loss of available cooling due to decrease in the surface area to volume ratio in low aspect ratio storage tanks. The discharge temperature of the water (temperature at $X = 1$) slightly increases with the decrease in aspect ratio for the same amount of fluid charged in each tank, i.e. the thermal stratification decreases with the decrease in the aspect ratio of the storage tank.

The effect of initial temperature difference on thermal stratification during a discharge cycle is shown in Fig. 24. The thermocline degradation increases with the increase in the initial temperature difference due to enhanced axial wall conduction and thermal diffusion between warm and cold water.

5. Conclusions

This study contributes to the understanding of the influence of various parameters controlling the thermal stratification in static and dynamic modes of operation of chilled water tanks. Mere insulation of the exterior surfaces to reduce heat exchange between ambient and stored fluid will not help in improving the thermal stratification as this may lead to increased thermal degradation due to axial wall conduction. This effect can be reduced by increasing the length and decreasing the thickness of the storage tank wall and also using a material of low thermal conductivity. Hence thermal stratification increases with the modified Biot number defined in this paper.

In storage tanks of small storage volumes a long storage tank may be preferable if there is no restriction on the maximum length. However, stratification does not improve markedly beyond an aspect ratio of 3.0. Similarly, not much advantage in thermal stratification is obtained beyond L/δ value of 200 for a storage tank irrespective of aspect ratio.

In tanks of large volumes, where there is a limitation on the height of the storage tanks, thermal stratification is possible even in tanks of low aspect ratio by adapting a small surface area to volume ratio and a large heat capacity ratio.

Thermal degradation increases with increase in Peclet numbers (charge and discharge flow rates) due to mixing at the inlets and outlets.

The material of the storage tank is found to have very little effect in the formation of thermoclines during charging (Fig. 14) and discharging (Fig. 21). In dynamic mode of operation the effects of mixing overtake the influence of other parameters. However the effect of wall material cannot be neglected in static storage systems wherein the tank is allowed to be idle with no in-flow and out-flows.

References

- [1] D.P. Fiorino, Case study of a large, naturally stratified, chilled water thermal energy storage system, *ASHRAE Trans* 97 (2) (1991) 1161–1169.
- [2] D.P. Fiorino, Energy conservation with thermally stratified chilled water storage, *ASHRAE Trans* 100 (1) (1994) 1754–1765.
- [3] S.P. Gretarson, C.O. Pedersen, R.K. Strand, Development of a fundamentally based stratified thermal storage tank model for energy calculation, *ASHRAE Trans* 100 (1) (1994) 1213–1220.
- [4] C.R. Truman, M.W. Wildin, Finite difference model for heat transfer in a stratified thermal storage tank with through flow, *Numerical heat transfer with personal computers and super computing*, ASME/AIChE National Heat transfer Conference, Philadelphia, Aug. 6–9 (1989) 45–55.
- [5] H. Yoo, E.T. Pak, Theoretical model of the charging process for stratified thermal storage tanks, *Solar Energy* 51 (1993) 513–519.
- [6] Nimr M.A. Al-, Temperature distribution inside a solar collector storage tank of finite thickness, *Trans ASME, Jnl of Solar Energy Engg* 115 (1993) 112–116.
- [7] J.E.B. Nelson A.R. Balakrisnan, S. Srinivasa Murthy, Experiments on stratified chilled water tanks, *Int. Journal of Refrigeration* submitted.

Appendix A

A.1. Discharge cycle

Energy balance in the element at “*t*”:

Energy degraded in the element (E_s) = Energy entering (E_1) – Energy leaving (E_2).

The energy balance in the fluid very close to the top of the storage tank (Fig. 2(a)) gives:

$$\rho_f c_f A \Delta x \frac{\partial T_t}{\partial t} = k_f A \frac{\partial T_t}{\partial x} + h_t A (T_\infty - T_t) + \dot{m} c_f (T_d - T_{m,1}) \quad (\text{A.1})$$

($T_d - T_{m,1}$) where $T_{m,1}$ is the temperature in the elemental volume after the inlet streams from the top and adjacent element mix with the fluid in the element “*t*” under consideration.

$$T_{m,1} = \frac{(C_1 = \dot{m} c_f \Delta t) T_d + (C_2 = m_{1,d} c_f) T_t}{C_1 + C_2}, \quad (\text{A.2})$$

where $m_{1,d}$ represents the amount of fluid in the element “*t*” mixing with the inlet stream entering through the top of the tank during the time interval Δt .

In the limit $\Delta x \rightarrow 0$ equation (A.1) simplifies to:

$$\frac{\partial T_t}{\partial x} + \frac{h_t}{k_f} (T_\infty - T_t) + \frac{\dot{m} c_f}{K_f A} (T_d - T_{m,1}) = 0. \quad (\text{A.3})$$

On substitution of equation (A.2) the above equation simplifies to:

$$\frac{\partial T_t}{\partial x} + \frac{h_t}{k_f} (T_\infty - T_d) + \frac{\dot{m} c_f}{K_f A Z_1} (T_d - T_{m,1}) = 0, \quad (\text{A.4})$$

where

$$Z_1 = \frac{C_1 + C_2}{C_2}.$$

Energy balance in the element “*b*” at $x = L$:

Energy stored/degraded (E_b) = Energy in (E_3) – Energy out (E_4).

$$\rho_f A C_f \frac{\partial T_b}{\partial t} = -k_f A \frac{\partial T_b}{\partial x} + h_b A (T_\infty - T_b) + \dot{m} c_f (T_N - T_{n,2}). \quad (\text{A.5})$$

In the limit as $\Delta x \rightarrow 0$ the equation (A.5) simplifies to:

$$\frac{\partial T_b}{\partial x} - \frac{h_b}{k_f} (T_\infty - T_b) - \frac{\dot{m} c_f}{k_f A} (T_N - T_{n,2}) = 0, \quad (\text{A.6})$$

where $m_{2,d}$ represents the mass of water in the element “*b*” mixing with the inlet stream from the top of the tank in time period Δt .

$$T_{n,2} = \frac{(C_7 = \dot{m} c_f \Delta t) T_N + (C_8 = m_{2,d} c_f) T_b}{C_7 + C_8}, \quad (\text{A.7})$$

$$\frac{\partial T_b}{\partial x} - \frac{h_b}{k_f} (T_\infty - T_b) - \frac{\dot{m} c_f}{k_f A Z_4} (T_N - T_b) = 0, \quad (\text{A.8})$$

where

$$Z_4 = \frac{C_7 + C_8}{C_8}.$$

The above equations are nondimensionalized using the dimensionless parameters given in the nomenclature. The mixing of the fluid may also take place in the nodes located next to the inlet on the downstream side depending on the velocity of the inlet jet. The temperature of mixing in the node under consideration is calculated from the following formula:

$$\theta_{i,\text{new}} = \frac{\theta_i + Z_{\text{int}} \theta_{i-1}}{Z_i + 1}. \quad (\text{A.9})$$

A.2. Charge cycle

Energy balance in the element at “*t*”:

Energy degraded in the element (E_s) = Energy entering (E_1) – Energy leaving (E_2).

The energy balance in the fluid very close to the top of the storage tank (Fig. 2(a)) gives:

$$\rho_f c_f A \Delta x \frac{\partial T_t}{\partial t} = k_f A \frac{\partial T_t}{\partial x} + h_t A (T_\infty - T_t) + \dot{m} c_f (T_1 - T_{m,2}) \quad (\text{A.10})$$

where $T_{m,2}$ is the temperatures in the elemental volume after the inlet stream from the node 1 mix with the fluid in the element “*t*” under consideration.

$$T_{m,2} = \frac{(C_3 = \dot{m} c_f \Delta t) T_1 + (C_4 = m_{1,u} c_f) T_t}{C_3 + C_4}, \quad (\text{A.11})$$

where $m_{1,u}$ represents the amount of fluid in the element “*t*” mixing with the inlet stream entering through the node 1 of the tank during the time interval Δt .

In the limit $\Delta x \rightarrow 0$ equation (A.1) simplifies to:

$$\frac{\partial T_t}{\partial x} + \frac{h_t}{k_f} (T_\infty - T_t) + \frac{\dot{m} c_f}{K_f A} (T_1 - T_{m,2}) = 0. \quad (\text{A.12})$$

On substitution of equation (A.11) the above equation simplifies to:

$$\frac{\partial T_t}{\partial x} + \frac{h_t}{k_f} (T_\infty - T_t) - \frac{\dot{m} c_f}{K_f A Z_2} (T_t - T_1) = 0, \quad (\text{A.13})$$

where

$$Z_2 = \frac{C_3 + C_4}{C_4}.$$

Energy balance in the element “b” at $x = L$:

Energy stored/degraded (E_b) = Energy in (E_3) – Energy out (E_4).

$$\rho_f A C_f \frac{\partial T_b}{\partial t} = -k_f A \frac{\partial T_b}{\partial x} + h_b A (T_\infty - T_b) + \dot{m} c_f (T_u - T_{n,1}) \quad (\text{A.14})$$

In the limit as $\Delta x \rightarrow 0$ the equation (A.14) simplifies to:

$$\frac{\partial T_b}{\partial x} - \frac{h_b}{k_f} (T_\infty - T_b) - \frac{\dot{m} c_f}{k_f A} (T_u - T_{n,1}) = 0, \quad (\text{A.15})$$

$$T_{n,1} = \frac{(C_5 = \dot{m} c_f \Delta t) T_u + (C_6 = m_{2,u} c_f) T_b}{C_5 + C_6}, \quad (\text{A.16})$$

where $m_{2,u}$ represents the mass of water in the element “b” mixing with the inlet stream from the top of the tank in time period Δt .

$$\frac{\partial T_b}{\partial x} - \frac{h_b}{k_f} (T_\infty - T_b) + \frac{\dot{m} c_f}{k_f A Z_3} (T_b - T_u) = 0, \quad (\text{A.17})$$

where

$$Z_3 = \frac{C_5 + C_6}{C_6}.$$

The mixing of the fluid may also take place in the nodes located next to the inlet on the downstream side depending on the velocity of the inlet jet. The temperature of mixing in the node under consideration is calculated from the following formula:

$$\theta_{i,\text{new}} = \frac{\theta_i + Z_{\text{int}} \theta_{i+1}}{Z_{i+1}}. \quad (\text{A.18})$$

The above equations are non-dimensionalized as given below:

$$\frac{\partial \theta}{\partial \tau} = \frac{\partial^2 \theta}{\partial X^2} - Pe \frac{\partial \theta}{\partial X} + S_i (\theta_w - \theta), \quad (\text{A.19})$$

$$\frac{\partial \theta_w}{\partial \tau} = \frac{\alpha_w}{\alpha_f} \frac{\partial^2 \theta_w}{\partial X^2} - \varepsilon S_i (\theta_w - \theta) + \varepsilon S_o \theta_w, \quad (\text{A.20})$$

with the initial condition

$$\theta(X, 0) = F(X). \quad (\text{A.21})$$

The boundary conditions are:

(a) *for static mode of operation:*

$$\frac{\partial \theta_t}{\partial X} + Bi_t \theta_t = 0, \quad (\text{A.22})$$

$$\frac{\partial \theta_b}{\partial X} + Bi_b \theta_b = 0; \quad (\text{A.23})$$

(b) *for charge cycle:*

$$\frac{\partial \theta_t}{\partial X} + Bi_t \theta_t - a_2(\theta_t - \theta_1) = 0, \quad (\text{A.24})$$

$$\frac{\partial \theta_b}{\partial X} - Bi_b \theta_b - a_2(\theta_u - \theta_N) = 0; \quad (\text{A.25})$$

(c) *for discharge cycle*

$$\frac{\partial \theta_t}{\partial X} + Bi_t \theta_t + a_1(\theta_d - \theta_t) = 0, \quad (\text{A.26})$$

$$\frac{\partial \theta_b}{\partial X} - Bi_b \theta_b - a_1(\theta_N - \theta_b) = 0. \quad (\text{A.27})$$